

STIMULATED RAMAN SCATTERING OF LIGHT

V. A. ZUBOV, M. M. SUSHCHINSKIĬ, and I. K. SHUVALOV

Usp. Fiz. Nauk 83, 197-222 (June, 1964)

1. INTRODUCTION

THE development of optical masers has led to the discovery of a new phenomenon—stimulated Raman scattering of light. This effect combines the characteristic features both of ordinary Raman scattering and of laser emission.

It is well known that in ordinary Raman scattering radiation of frequency ν is transformed into radiation having a complex spectral character in which in addition to the frequency ν the frequencies $\nu \pm \nu_R$ are also present. Here the ν_R are frequencies characteristic of the scatterer and are usually normal vibrational or rotational frequencies of the molecules of the material under study.

The phenomenon of Raman scattering can be clearly understood in terms of a modulation of the incident light wave of frequency ν by the normal vibrations of the scattering substance or material at frequencies ν_R . It was precisely this concept of modulation which led L. I. Mandelshtam and G. S. Landsberg to the discovery of Raman scattering.^[1]

The phenomenon of modulation is also fundamental to stimulated Raman scattering, which was discovered by Woodbury and Ng in 1962 while working with giant ruby laser pulses^[2]. They used an optical shutter consisting of a nitrobenzene-filled Kerr cell to decrease the pulse length of the ruby laser. It was discovered that the output of the laser included additional frequencies which were characteristic of the Raman scattering of nitrobenzene; the intensity of the emission at these additional frequencies was very large.

Although stimulated Raman emission was discovered accidentally in the experiments of Woodbury and Ng, it should be pointed out that the effect had been predicted several years previously. In fact Javan^[3] pointed out in 1958 that two photon processes could be used to amplify light without requiring population inversion of energy levels.

Since the work of Woodbury and Ng a number of papers on stimulated Raman emission have appeared^[3-8] describing various characteristic features of the phenomenon. The possibility of practical applications of the effect has also been pointed out.

2. BASIC EXPERIMENTAL RESULTS

A. Scatterer Inside the Laser Cavity

Woodbury and Ng discovered stimulated Raman emission in nitrobenzene. These experiments were later continued in more detail by Eckhart and others^[4]. These authors investigated a long list of substances and showed that the radiation at the shifted frequencies was stimulated Raman scattering.

The following arrangement was used in^[4] (Fig. 1). The laser was a cylindrical ruby rod with a polished surface and of dimensions 76×9.5 mm. The pump source was a coiled flash lamp. Multilayer dielectric mirrors were used in the cavity. A quartz Wollaston prism served as a polarizer. The switching element was a Kerr cell in which the nitrobenzene was replaced by a KH_2PO_4 crystal, which does not contribute lines of its own. The cell containing the material being studied was from 2.5 to 10 cm. long and was inside the ruby laser cavity. This was done both because the pumping line at 6943 \AA is much stronger inside the cavity and also because the same cavity served both for the ruby emission and for the stimulated emission from the substance. The light output was collected from both ends of the cavity. A photomultiplier for monitoring the ruby line at 6943 \AA was placed at one end and a spectrograph was placed at the other end; detection was either by film or by a photomultiplier which could be moved in the focal plane of the spectrograph. This setup was used to record the emission from the test substance. The ruby output pulse power was from 0.2 to 2 MW in a spike 20–70 nsec long, corresponding to an energy between 0.05 and 0.2 J.

The results obtained by the authors in^[4] for the frequency shifts in the emission from liquids relative to the frequency of the ruby laser are shown in Table I. The table also lists the frequencies of the strongest lines in the Raman scattering from these same substances. The results obtained in^[4] refer only to substances with ring structures with five or more CH or CD groups.

The authors point to three effects which indicate the existence of coherent oscillation at the shifted frequencies. The first is the high degree of parallelism of the

FIG. 1. Experimental set-up. 1) photomultiplier; 2) multilayer dielectric mirror; 3) Kerr cell; 4) polarizer; 5) ruby rod; 6) cuvette containing investigated liquid; 7) condensing lens; 8) entrance slit of the spectrograph.

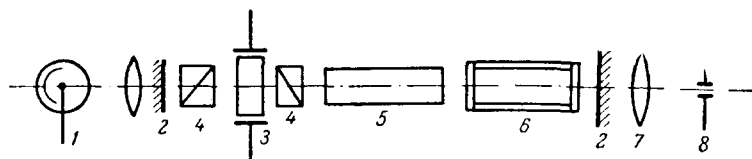


Table I

Substance	Displacement of the emission frequency of the liquid relative to the ruby frequency in cm^{-1}	Frequencies of the strongest lines of the Raman scattering in cm^{-1}	Вещество	Displacement of the emission frequency of the liquid relative to the ruby frequency in cm^{-1}	Frequencies of the strongest lines of the Raman scattering in cm^{-1}
Benzene	990 ± 2	992	Pyride	992 ± 2	991
	$2 \times (990 \pm 2)$ 3064 ± 4	3064		$2 \times (992 \pm 5)$	3054
Nitrobenzene	—	1004	Cyclohexane	—	801
	1344 ± 2	1345		2852 ± 1	2853
	$2 \times (1346 \pm 2)$ $3 \times (1340 \pm 5)$	—	Deuterobenzene	944 ± 1	945
Toluene	—	785		$2 \times (944 \pm 1)$	2292
	1004 ± 4	1002		—	—
1-Bromo-naphthalene	1368 ± 4	1363			
	—	3060			

output beam, which is the same as that of the ruby laser output. The second is the line narrowing of the output, which becomes more pronounced as the energy of the pumping beam is increased. The line width was as small as 0.6 cm^{-1} , compared to 10 cm^{-1} in ordinary Raman scattering. Third, there is a threshold value of the pump energy, or more precisely a threshold value of the output power of the ruby laser corresponding to a given length of the cell for the investigated substance, i.e., there is a threshold value for the laser power, depending on the length of the light path in the active medium.

Eckhart et al. established the following features of the stimulated Raman effect.

1. As the threshold is exceeded the output power increases rapidly and becomes as large as 0.01–0.1 times the power of the primary laser pumping beam, i.e., as large as 10–100 kW.

2. The shift of the output frequencies from the frequency of the pumping line was in agreement with the vibrational frequencies observed in the Raman spectra of the materials studied.

3. The emission was observed to consist of only one displaced line or in several cases of lines whose frequency shifts were multiples of a given shift. In other words if a line appears having a frequency shift ν_R , then in certain cases lines displaced by frequencies $2\nu_R$, $3\nu_R$ were also observed (cf. Table I).

4. Stimulated emission was observed only in lines corresponding to the strongest lines in the ordinary Raman spectrum.

5. The shifted emission lines were observed only in the Stokes region.

It does not seem possible to relate the observed effects to the absorption of energy from the primary beam followed by subsequent emission, as is possible with two independent processes. For example the absorption in benzene and deuterobenzene differs significantly at 6943 \AA (benzene has an absorption coeffi-

cient 0.02 cm^{-1} , deuterobenzene 0.001 cm^{-1}); however the energies of the emissions in the two cases are essentially identical. It is therefore much more probable to ascribe the observed effects to stimulated Raman scattering.

The authors explain the appearance of the second and third Stokes shifted frequencies by repeated process of stimulated Raman scattering caused by the lines already excited, i.e., oscillation in the first line acts as a pump to produce stimulated emission in the second line.

More recent results concerning stimulated Raman scattering have been published by Geller et al.^[5] Their experimental arrangement was similar to that shown in Table II. The criteria for stimulated emission used by these authors were first the high parallelism of the output beam and second the existence of

Table II

Substance	Displacement of the emission frequency of the liquid relative to the ruby frequency in cm^{-1}	Frequencies of the strongest lines of the Raman scattering in cm^{-1}
Ethylbenzene,	1002 ± 10	1000
Acetone	2921 ± 7	2922
Cyclohexanone	2863 ± 7	2949
Pipridine*	2945 ± 5	2935
	2933	
	2936	
	2940	
	2943	
p-Xylene	2998 ± 14	3008
m-Xylene	2933 ± 10	2916
o-Xylene*	2913	2916
	2922	
	2933	
	730	733

Note *Sample radiates a multiplet.

a threshold value of the ruby laser power. The output radiation was observed to have the following characteristics.

1. A strong suppression effect occurs, i.e., if two or more substances which are Raman active are present, stimulated Raman emission in the weaker lines is prevented by stimulated emission in the stronger lines. The authors relate this to the decrease in the power of the primary laser beam due to the transfer of energy into the Raman scattered beam.

2. Several liquids (denoted by asterisks in Table II) exhibited emission in the form of narrow, closely spaced lines. The separations between these lines are comparable with those which are observed in rotational spectra.

Because of the high threshold associated with stimulated Raman scattering it was originally observed only with Q-switched lasers; recently however the effect has been observed using an ordinary ruby laser even though the ordinary ruby laser is about two orders of magnitude less powerful than a Q-switched laser. However because of the longer duration of the pumping action it is possible to reach the oscillation threshold of the shifted line. The experimental setup used in [6] was similar to that used in [2-5].

The ruby laser used had a pump energy threshold of 270 joules. Expressed in terms of the pump energy for the ruby laser, the threshold for stimulated emission was 360 joules. The duration of the spikes was about 500 μ sec. The criteria for laser action at the shifted frequencies were, as usual: 1) the line narrowing observed in stimulated Raman emission compared with the lines observed in usual Raman spectra; 2) the high degree of parallelism of the beam; 3) the presence of an oscillation threshold. Under the above conditions oscillation was obtained at one of the strongest of all Raman lines, the benzene line at 992 cm^{-1} .

B. The Scatterer Outside the Laser Cavity

All of the above papers dealt with the observation of stimulated Raman scattering in the Stokes region. Recent papers by Terhune [7] and Stoicheff [8], using both organic liquids and materials more complicated to deal with experimentally (liquified gases, gases under pressure, etc), supported the previous results. Moreover these papers reported the observation of stimulated emission at wavelengths shorter than 6943 \AA , i.e., in the anti-Stokes region.

Stoicheff [8] used the experimental arrangement of Fig. 2. A ruby laser served as the light source. A rotating prism acted as a Q-switch. Its rate of rotation was 400 cps. The flash lamp was synchronized with the rotating prism. A multilayer dielectric mirror was used in the cavity. The energy emitted in the ruby line at 6943 \AA varied from 0.1 to 0.8 joules. The length of the giant pulse was about 20 nanoseconds. To obtain the maximum power density the laser radiation was

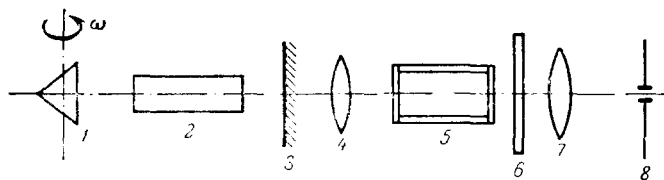


FIG. 2. Experimental set-up. 1) rotating totally reflecting prism; 2) ruby rod; 3) multilayer dielectric mirror; 4) lens with 25-cm focal length; 5) cuvette containing liquid under study; 6) filter; 7) condensing lens; 8) entrance slit of the spectrograph.

focused by a lens of 25 cm. focal length into a cuvette containing the liquid being studied. The length of the cuvette was varied between 2 and 70 mm. The cross section of the laser beam in the cuvette did not exceed 0.1 cm^2 . Under these conditions the power density was estimated to be about 100 MW/cm^2 and higher. A color filter was placed behind the cuvette to absorb the exciting radiation. A similar apparatus was used in [7] for exciting stimulated emission.

It should be pointed out that, in contrast to the papers discussed in Sec. A above, the liquid studied was located outside the ruby laser cavity. On the one hand this raised the requirement on the power from the exciting laser pulse, since the energy density outside the cavity is significantly smaller than inside. On the other hand this experimental arrangement allowed one to investigate the radiation coming out of the liquid over a wide range of angles, which turned out (as will be seen) to be very important.

When the emission from the liquid was photographed on color reversal film placed some distance from the cuvette, a rather unexpected picture was obtained. The photographs showed concentric rings corresponding to red, orange, yellow, and green light. It must be remembered that infrared radiation does not affect color film. A color reproduction of the observed picture is reproduced by A. L. Schawlow [Sci. American 209(1), 34 (1963)]. A more detailed investigation showed that these rings are related to the anti-Stokes components of the usual Raman scattering.

In studying the spectrum of the scattered radiation, spectrographs both with small dispersion (to obtain the overall spectrum) and with large dispersion and resolution (to obtain more detail) have been used.

Investigation of the spectrum of the radiation emitted from a number of liquids allows one to conclude the following. The spectra are extremely intense; a single pulse from the pumping laser is sufficient to expose a spectrogram. The spectra contain Stokes and anti-Stokes lines of almost the same intensity; moreover each spectrum contains not only lines shifted by the fundamental frequency but also lines shifted by frequencies which are exact multiples of the basic frequency shift.

More detailed study has led to a number of interesting conclusions.

1. There is a threshold for the appearance of radi-

ation at the shifted frequency both in terms of the power in the exciting beam and in terms of the length of the light beam in the liquid. Moreover as soon as the threshold is exceeded by only a very small amount the whole set of displaced frequencies appears, i.e., lines shifted by the primary interval as well as lines shifted by the harmonics both in the Stokes and in the anti-Stokes regions. In other words the threshold for exciting the shifted lines is the same both for the fundamental and for the harmonics and is the same both for the Stokes and for the anti-Stokes regions. Near threshold the intensity of typical lines is several per cent of the intensity of the exciting radiation.

2. The magnitude of the threshold is related both to the intensity and line width of ordinary Raman scattering. As an illustration we will compare the ordinary Raman spectra of carbon disulfide, benzene, and carbon tetrachloride. The relative intensities of the strongest lines of these materials are approximately in the ratio 5:4:1, and the line widths of the same materials are 1.0, 2.5, and 2 cm^{-1} respectively. Correspondingly, experiment shows that the lowest threshold for stimulated Raman emission occurs in carbon disulfide, whereas the highest is carbon tetrachloride.

3. For each liquid the frequency-shifted radiation contains only one or two lines and their harmonics; the frequencies of these lines correspond to totally symmetric vibrations in the ordinary Raman spectrum. This result is understandable since it is precisely these vibrations which give the narrowest and most intense lines in ordinary Raman scattering, and hence these lines have the lowest threshold (cf. above). Comparison of the frequencies obtained in these experiments with the frequencies of the lines in the ordinary Raman spectrum show that, within the limits of error of the experiment (about 0.2 cm^{-1}), the frequencies are equal. The Stokes and anti-Stokes frequencies also agree to within the limits of error of measurement (about 0.3 cm^{-1}). The frequencies of the harmonics are equal to twice, three times, and four times the fundamental frequency to within an error of about 0.3 cm^{-1} . These harmonics in the Raman scattering do not have analogs in the ordinary Raman scattering spectrum. In fact the overtone lines of molecular vibrations usually have intensities orders of magnitude smaller than the lines of fundamental vibrations. Moreover the frequencies of these overtone lines are not exactly equal to twice, three times, etc. the frequencies of the primary vibration due to the anharmonicity of the vibrations. All the evidence indicates that these harmonics cannot be attributed to a repetitive process; i.e., they are not produced from the first Stokes line in the way that the first Stokes line was produced from the exciting laser beam. This follows from experiments in which a sequence of two liquids was placed in the output beam of the laser (in the particular case studied the cells were filled with carbon disulfide and benzene); the order in which the beam

Table III

Substance	Angles at which anti-Stokes radiation is observed
Benzene	$2^{\circ}48'$ $4^{\circ}30'$
CS ₂	$3^{\circ}19'$ $4^{\circ}54'$
Toluene	$2^{\circ}54'$
Nitrobenzene	$3^{\circ}30'$
Nitrogen (liquid)	$1^{\circ}10'$

went through the two liquids could be changed. The harmonics of each liquid were observed in these experiments (it should be pointed out however that the spectrum of CS₂ was usually predominant) but there was a complete absence of lines corresponding to the sum and difference frequencies of the Raman lines of these liquids, although such lines might be expected on the basis of a repetitive process. Further evidence consists in the fact that as soon as threshold is exceeded by a small amount the harmonic lines appear simultaneously with the primary line.

4. Investigation of the angular distribution of the frequency shifted radiation over a range of 40° showed that the Stokes emission is strongest within angles of $4-5^{\circ}$ around the forward direction and then falls off rapidly. A similar maximum in the Stokes emission was also observed in the back direction, but its intensity was an order of magnitude smaller. The situation is different for the anti-Stokes emission. This emission occurs only at well defined angles with respect to the direction of propagation of the exciting radiation. This angle, which has been determined to an accuracy of about $10'$, amounts to several degrees to the direction of propagation of the excited light depending on the material and the order of the harmonics (Table III). This of course is responsible for the appearance of colored rings when the emission from a liquid is recorded on color film (the film is not sensitive to the Stokes emission). The authors explain the scattering of light at definite angles by the laws of conservation of momentum during light scattering (cf. Sec. 3).

5. Investigation of the widths of the Stokes lines in the scattered radiation for several liquids showed that they are much narrower than the widths of the corresponding lines in ordinary Raman scattering. Significant line narrowing was also observed in the anti-Stokes region. Measurement of the width of the first line in benzene, made with a Fabry-Perot interferometer, gave a width of about 0.05 cm^{-1} , whereas in ordinary Raman scattering the width is about 2.5 cm^{-1} .

All of these previously cited characteristics of the frequency shifted emission allow one to conclude that

it is stimulated Raman scattering. The fact that the anti-Stokes lines were not observed when the scattering material was placed inside the resonator is explained by the experimental circumstances. The anti-Stokes component could not be observed because of the presence of a cavity tuned to radiation along the axis of the cavity and because the components of the anti-Stokes emission are emitted at an angle to the axis.

Mention should be made of certain other facts which were established experimentally in the papers cited.

1. When the stimulated emission spectrum exhibits a strong anti-Stokes line corresponding to a change in a vibrational quantum number $1 \rightarrow 0$ there is a complete absence of the Stokes line corresponding to a transition from the same initial level, i.e., the vibrational transition $1 \rightarrow 2$. We note that according to both theory and experiment in ordinary Raman scattering these Stokes lines should have somewhat larger intensity than the anti-Stokes lines corresponding to the vibrational transition $1 \rightarrow 0$.

2. Usually the output of the ruby laser contains a single narrow line, but sometimes the emission contains two lines separated by 0.8 cm^{-1} . In this case the stimulated Raman line has a distinctive form. In the Stokes region the primary line in the stimulated Raman emission is somewhat broadened. The second and third harmonics of the primary line have widths which are correspondingly 2 and 3 times greater and the shape of these lines is asymmetric. The maximum is displaced towards the high frequency side, i.e., towards the exciting line. In the anti-Stokes region the primary line and the harmonics are similarly broadened and anti-symmetric and the maximum is also displaced towards the high frequencies, i.e., away from the exciting line. It was established that within the broadened primary anti-Stokes line there is a deep and narrow gap whose width is about 0.2 cm^{-1} . This gap is somewhat displaced (about 0.2 cm^{-1}) from the position of the maximum when the spectrum is observed with a ruby laser exhibiting a single line. In several cases, under analogous excitation conditions, the spectrum of the stimulated Raman scattering contained instead of a line a whole series of maxima. The separation between the maxima was equal to the separation between the exciting lines. The total width of such a series was several angstroms.

We should mention particularly the production and investigation of stimulated Raman scattering in liquified gases. Intense anti-Stokes scattering from liquid hydrogen, oxygen and nitrogen was reported in [8]. It should be pointed out that in ordinary Raman scattering anti-Stokes emission has not been seen in any of these cases and would not be expected because of the very low temperature. The character of the observed spectra is completely similar to that obtained with organic liquids.

The spectrum of liquid hydrogen was studied especially in the hope of obtaining stimulated Raman scattering

corresponding to molecular rotations, since in ordinary Raman scattering from gaseous and liquid hydrogen the rotational lines are somewhat more intense than the vibrational lines. The line widths in the two cases are essentially the same. However they succeeded experimentally in observing only lines corresponding to the transition $v=0 \rightarrow v=1$, $I=0 \rightarrow I=0$, where v and I are the vibrational and rotational quantum numbers. The authors suggest that in the process of stimulated Raman scattering only transitions with $\Delta I = 0$ occur; in other words, stimulated Raman scattering is predominantly isotropic rather than anisotropic.

3. THE THEORY OF STIMULATED RAMAN SCATTERING

A. Semiclassical Theory

The most important features of the phenomenon of stimulated Raman scattering may be understood from a semiclassical consideration. The general outline of this treatment has been given by Townes [9,10].

Following these latter references, we consider a molecule with polarizability α in an electric field \mathbf{E} . Under the influence of the field \mathbf{E} the molecule develops an electric moment $\mu = \alpha \mathbf{E}$ and a potential energy $U = -\alpha \mathbf{E}^2/2$.

Let x be the vibration coordinate describing a particular vibration of the molecule. Considering the molecule to be acted on by the driving force

$$F = -\frac{dU}{dx} = \frac{1}{2} \frac{d\alpha}{dx} \mathbf{E}^2, \quad (1)$$

we obtain the equation for the internal molecular vibration

$$m\ddot{x} + R_0\dot{x} + fx = F_0 \cos \omega t \quad (2)$$

(the driving force is assumed to be harmonic). The solution of this equation for a frequency ω close to the resonance frequency $\omega_r = \sqrt{f/m}$ is

$$x = \frac{F_0}{R_0\omega} \sin \omega t. \quad (3)$$

Let R_0 be a phenomenological damping constant, and f the quasielastic force constant of the molecule corresponding to the normal vibration ω_r .

We now assume that the electric field \mathbf{E} is the sum of several plane waves differing in frequency by the amount ω or (in a more general case) by a frequency which is a multiple of ω . In the simplest case of two such waves we have

$$\mathbf{E} = \mathbf{E}_0 e^{i(\omega_0 t - \mathbf{k}_0 \cdot \mathbf{r})} + \mathbf{E}' e^{i(\omega' t - \mathbf{k}' \cdot \mathbf{r} + \varphi)}, \quad (4)$$

where $\omega_0 - \omega' = \omega$. We then have

$$\mathbf{E}^2 = \mathbf{E}_0^2 + \mathbf{E}'^2 + 2\mathbf{E}_0 \mathbf{E}' \cos [(\omega_0 - \omega') t - (\mathbf{k}_0 - \mathbf{k}') \cdot \mathbf{r} - \varphi]. \quad (5)$$

The constant terms may be discarded and we obtain

$$F_0 = \frac{d\alpha}{dx} \mathbf{E}_0 \mathbf{E}'. \quad (6)$$

Correspondingly we have

$$x = \frac{E_0 E' \frac{d\alpha}{dx}}{R_0 (\omega_0 - \omega')} \sin [(\omega_0 - \omega') t - (\mathbf{k}_0 - \mathbf{k}') \mathbf{r} - \varphi']. \quad (7)$$

The molecular vibration gives rise to an oscillating dipole moment

$$\begin{aligned} \boldsymbol{\mu} = x \frac{d\alpha}{dx} \mathbf{E} &= \frac{E_0 E' \left(\frac{d\alpha}{dx} \right)^2}{R_0 (\omega_0 - \omega')} \\ &\times \{ \sin [(\omega_0 - \omega') t - (\mathbf{k}_0 - \mathbf{k}') \mathbf{r} - \varphi'] \} \mathbf{E}. \end{aligned} \quad (8)$$

The rate of exchange of energy between the dipole moment and the component of the field at frequency ω' is given by the formula

$$P' = - \left\langle \frac{d\boldsymbol{\mu}}{dt} \mathbf{E}' \right\rangle, \quad (9)$$

where the average is taken with respect to time. From this we obtain the power which is transferred to the component \mathbf{E}' from the initial beam \mathbf{E}_0 :

$$P' = \frac{1}{2R_0} \left(\frac{d\alpha}{dx} \right)^2 \frac{\omega'}{\omega_0 - \omega'} (E_0 \mathbf{E}')^2. \quad (10)$$

For Stokes lines $\omega' = \omega_0 - \omega_r$, $P' > 0$ and the radiation corresponding to the component \mathbf{E}' is amplified. For anti-Stokes radiation $\omega' = \omega_0 + \omega_r$ and this component loses energy.

In order to be able to explain the possibility of oscillation at the anti-Stokes line we consider the case in which the field \mathbf{E} has three components with different frequencies:

$$\begin{aligned} \mathbf{E} = & E_0 e^{i(\omega_0 t - \mathbf{k}_0 \mathbf{r})} + E_{-1} e^{i[(\omega_0 - \omega_r) t - \mathbf{k}_{-1} \mathbf{r} + \varphi_{-1}]} \\ & + E_{+1} e^{i[(\omega_0 + \omega_r) t - \mathbf{k}_{+1} \mathbf{r} + \varphi_{+1}]}. \end{aligned} \quad (11)$$

Using the previous method we can calculate the vibration of the molecule and its oscillating dipole moment. From this we obtain a power amplification of the Stokes emission

$$\begin{aligned} P_{-1} = & \frac{1}{2R_0} \left(\frac{d\alpha}{dx} \right)^2 \frac{\omega_0 - \omega_r}{\omega_r} \{ (E_0 E_{-1})^2 \\ & - (E_0 E_{+1}) (E_0 E_{-1}) \cos [(2\mathbf{k}_0 - \mathbf{k}_1 - \mathbf{k}_{-1}) \mathbf{r} + \varphi_1 + \varphi_{-1}] \}. \end{aligned} \quad (12)$$

The power gain in the anti-Stokes wave will be

$$\begin{aligned} P_{+1} = & \frac{1}{2R_0} \left(\frac{d\alpha}{dx} \right)^2 \frac{\omega_0 + \omega_r}{\omega_r} \{ - (E_0 E_{+1})^2 \\ & - (E_0 E_{+1}) (E_0 E_{-1}) \cos [(2\mathbf{k}_0 - \mathbf{k}_1 - \mathbf{k}_{-1}) \mathbf{r} + \varphi_1 + \varphi_{-1}] \}. \end{aligned} \quad (13)$$

Thus if $|E_{-1}| > |E_{+1}|$, the component \mathbf{E}_{+1} will be amplified provided the following conditions are satisfied

$$2\mathbf{k}_0 = \mathbf{k}_1 + \mathbf{k}_{-1} \text{ and } \cos(\varphi_1 + \varphi_{-1}) < 0. \quad (14)$$

Here \mathbf{k}_0 , \mathbf{k}_{-1} and \mathbf{k}_1 are the wave vectors of the incident, the Stokes and the anti-Stokes waves respectively. If $\varphi_1 + \varphi_{-1} = \pi$ the gain at the anti-Stokes line will be greater. Under these conditions the gain at the Stokes line will decrease in the same direction because of the negative sign of the cosine term.

Oscillation at the Stokes and anti-Stokes Raman

lines may be understood qualitatively from the point of view of the modulation of the incident light wave by the coherent vibrations of the molecules. In fact numerical estimates show that a ruby pulse with a power of the order of 100 MW/cm² can cause an expansion and contraction in the length of molecular bonds of the order of 10⁻⁴ of their equilibrium value. In the scattering volume this gives rise to elastic waves with a frequency equal to the eigenfrequency ω_r of the molecular vibration. In the planes of constant phase of such a wave all of the molecules are vibrating synchronously with a given phase, which causes an expansion and compression of the medium. The concurrent relative change in the dielectric constant is about 10⁻⁴. These spatial variations in the dielectric act as a phase grating which scatters light waves. Since the variation in the dielectric constant depends on time, modulation of the light wave will occur with the formation of sidebands at frequencies $\omega_0 \pm m\omega_r$, where $m = 1, 2, 3, \dots$. Clearly this modulation mechanism is the same in principle as the modulation of light by hypersonic waves of thermal origin. Thus we have returned to the initial ideas of L. I. Mandel'shtam which are fundamental to ordinary Raman scattering. It should be noted that the waves we have described are not established as rapidly as the vibrations of the molecules themselves. The time for establishing elastic waves is of the order of 10⁻⁹ sec.

There are no additional conditions on the wave vectors involved in emission in the Stokes lines, and therefore Stokes emission may occur in all directions. In contrast to this it follows from (14) that anti-Stokes emission may occur only in directions forming a cone of angle θ_1 with respect to the direction of the initial light beam. For small angles θ_1 direct calculation gives

$$\theta_1^2 \approx \frac{1}{n} \frac{\omega_0 - \omega_r}{\omega_0 + \omega_r} \left[\Delta n_1 - \Delta n_{-1} + \frac{\omega_r}{\omega_0} (\Delta n_1 + \Delta n_{-1}) \right]. \quad (15)$$

Here n is the index of refraction of the medium at frequency ω_0 , Δn_1 and Δn_{-1} are the differences in the index of refraction at frequencies $\omega_0 \pm \omega_r$ and ω_0 respectively. For normal dispersion all of these quantities are positive. Since $\omega_r/\omega_0 \ll 1$, we obtain

$$\theta_1^2 \approx \frac{1}{n} \frac{\omega_0 - \omega_r}{\omega_0 + \omega_r} (\Delta n_1 - \Delta n_{-1}). \quad (16)$$

Thus the angle is determined by the slope of the dispersion curve of the medium. Numerical estimates show that these angles are of the order of a few degrees.

It is important that in order to generate anti-Stokes emission there is no additional threshold requirement which must be met once Stokes emission has been generated in the necessary direction. Furthermore in the presence of Stokes radiation at frequency $\omega_0 - \omega_r$ a field \mathbf{E}_{-2} can arise with frequency $\omega_0 - 2\omega_r$. The power radiated at this frequency consists of two parts. One of them is proportional to $\mathbf{E}_{-1}^2 \mathbf{E}_{-2}^2$ and may be ob-

tained by calculations analogous to those carried out previously. In addition there is a field at this frequency produced by modulating the field \mathbf{E}_1 by the vibrations of the dielectric susceptibility due to \mathbf{E}_0 and \mathbf{E}_{-1} . In this case the power generated is proportional to $|\mathbf{E}_0| |\mathbf{E}_{-1}|^2 |\mathbf{E}_{-2}|$. Since $|\mathbf{E}_{-2}| < |\mathbf{E}_0|$ this part of the radiation at frequency $\omega_0 - 2\omega_R$ may be largest only if an additional condition on the directions of the wave vectors is satisfied (cf. [9,10]). The higher harmonics in the Stokes region with frequencies $\omega_0 - m\omega_R$ are obtained analogously.

It should be pointed out that the first mechanism for the appearance of the frequency $\omega_0 - 2\omega_R$ involves attaining a well defined threshold, whereas the second does not. Correspondingly, the first mechanism in all probability operates when the liquid is placed inside the cavity, since the requirements on the wave vectors are not fulfilled there. The second mechanism may predominate when the liquid is placed outside the cavity, since the conditions on the wave vectors are fulfilled and there is no additional threshold requirement.

The harmonic in the anti-Stokes region with frequency $\omega_0 + 2\omega_R$ is produced without threshold requirements by a modulation of the frequency $\omega_0 + \omega_R$ by the vibrations at frequency ω_R . The radiation at this frequency is emitted in directions determined by the equation

$$\mathbf{k}_0 - \mathbf{k}_{-1} = \mathbf{k}_2 - \mathbf{k}_1. \quad (17)$$

The angle between \mathbf{k}_0 and \mathbf{k}_2 is approximately $2\theta_1$. The other anti-Stokes harmonics with frequencies $\omega_0 + m\omega_R$ are generated in analogous fashion in cones whose axes are along the direction of the initial beam.

Thus the semiclassical theory of Raman scattering provides an explanation of the basic features of this effect.

B. Quantum Theory of Stimulated Raman Scattering

Development of a quantum theory of stimulated Raman scattering has proceeded in several directions. Rivoire and Dupeyrat^[11] show that stimulated Raman scattering follows from the general formula of Plachek^[12]

$$W_{kn} = \frac{16\pi^4}{h^2} \sum_j \sum_{j'} \int \int \int \rho_j(\nu, O) \times \left\{ \frac{h\nu'}{c^3} + \rho_{j'}(\nu', O') \right\} |\mathcal{E}_{kn}^{aj'n'}|^2 d\nu dO dO'. \quad (18)$$

Here W_{kn} is the probability for Raman scattering to the frequency ν' due to excitation by a line of frequency ν , and the indices k, n indicate respectively the initial and final states of the molecules.

$\rho_j(\nu, O)d\nu dO$ is the energy density of the exciting radiation of polarization j emitted in the frequency interval $d\nu$ in the solid angle dO , and $\rho_{j'}(\nu', O')d\nu'dO'$ is the same quantity for the scattered radiation.

The first term in this equation represents "spontaneous" Raman scattering. The ratio of the anti-

Stokes and Stokes intensities is different for spontaneous and stimulated scattering:

$$\left(\frac{I_{as}}{I_s} \right)_{sp} = \left(\frac{\nu + \nu_{kn}}{\nu - \nu_{kn}} \right)^4 e^{-\frac{h\nu_{kn}}{kT}}, \quad (19)$$

$$\left(\frac{I_{as}}{I_s} \right)_{st} = \frac{(\nu + \nu_{kn}) \rho_{j'}(\nu + \nu_{kn}, O')}{(\nu - \nu_{kn}) \rho_{j'}(\nu - \nu_{kn}, O')} e^{-\frac{h\nu_{kn}}{kT}}. \quad (20)$$

Usually the cell containing the material to be investigated is placed in a Fabry-Perot resonator. The threshold for stimulated Raman scattering occurs when, because of the increase in the density $\rho(\nu', O')$ of the stimulated Raman scattered light, the gain at the scattered frequency compensates the losses in the cavity. If Π is the volume energy density in the cavity, and $\Delta\nu'$ is the average line width of the stimulated Raman scattering, then

$$\Pi = \rho(\nu') \Delta\nu'.$$

The energy losses are given by the expression

$$\frac{d\Pi}{dt} = \frac{\Pi(1-R)u}{l}. \quad (21)$$

Here R is the reflectivity of the interferometer plates, l is the separation between the plates, and u is the energy propagation velocity in the interferometer. The energy gain at the scattered frequency is given by

$$\frac{d\Pi}{dt} = N(W_{kn})_{st} h\nu', \quad (22)$$

where N is the number of molecules per unit volume in the initial state k within the interferometer. Threshold is attained when

$$N(W_{kn})_{st} \frac{h\nu'}{\Delta\nu'} = \frac{(1-R)u}{l} \rho(\nu'). \quad (23)$$

If P_{sp} is the spontaneously scattered power, and V is the radiating volume in the interferometer in the absence of the reflecting plates, then

$$P_{sp} = \frac{(1-R)u}{l} \frac{8\pi h}{\lambda'^3} \Delta\nu' V. \quad (24)$$

Numerical calculations using this formula show that the necessary value of the power P_{sp} may be obtained only for very powerful excitation sources.

Javan^[13] gives a quantum mechanical procedure for calculating stimulated Raman scattering. It involves essentially the same ideas considered in discussing the semiclassical theory of the effect. However description of the fundamental assumptions of the theory in quantum mechanical form permits one to gain a better understanding of certain features of the process.

We consider a two-level system which is acted on by two fields with frequencies Ω and ω , where $\omega < \Omega$. The frequency difference $\Omega - \omega$ equals $(E_n - E_i)/\hbar$, where E_n and E_i are the energies of the upper and lower levels. It is assumed that initially there are sufficient photons present both at ω and Ω to induce transitions from the lower state to the upper state (the photon of frequency Ω is absorbed and a photon of fre-

quency ω emitted) as well as the reverse transition (photon ω absorbed, photon Ω emitted). We assume that W_r is the rate of these two photon transitions (W_r is the same for transitions $i \rightarrow n$ and $n \rightarrow i$). The total power emitted at frequency ω is

$$P_i = (n_i - n_n) W_r \hbar \omega. \quad (25)$$

Thus we have power gain if the temperature is positive ($n_i > n_n$). This is a stimulated process and W_r is proportional to the total number of incident photons at frequencies Ω and ω . W_r is given by the expression

$$W_r = \frac{2\pi}{\hbar} |K_{if}|^2 \rho(\omega), \quad (26)$$

where $\rho(\omega)$ is the density of final states and

$$K_{if} = \sum_n \frac{\langle i | v | n \rangle \langle n | v | f \rangle}{E_i - E_n} \quad (27)$$

is the matrix element of the second order perturbation connecting the initial and final states summed over all intermediate states. If the pump frequency is absorbed over a band $\Delta\Omega$ then the gain will be determined by the half-width of the band $\Delta\Omega$, where $\Delta\Omega$ is a band of frequencies broader than the transition line width. In this case phase coherence is not important.

In the case of a coherent source the radiation field may be treated by classical theory. The emitted field $E e^{i\omega t}$ generates a polarization per unit volume

$$\gamma = \chi E e^{i\omega t}, \quad (28)$$

where $\chi = \chi' + i\chi''$ is the complex susceptibility. The average power emitted as a result of the interaction of the field with the polarization is

$$\Delta P = -\frac{1}{T} \operatorname{Re} \int_0^T \dot{\gamma} E dt = \frac{1}{2} \chi'' E_0^2 \omega, \quad (29)$$

where $T = 1/\omega$. If one assumes that all atoms are initially in the ground state and one divides ΔP by the number of atoms, then the transition rate is

$$W_r = \frac{\Delta P_a}{\hbar \omega} = \frac{1}{2} \chi_a'' E_0^2, \quad (30)$$

where χ_a'' is the susceptibility of a single atom.

The problem is solved with the help of the formal apparatus of density matrix ρ .

At least three levels are necessary for Raman scattering (Fig. 3). The initial (1) and final (3) states are not connected by any dipole matrix element. However

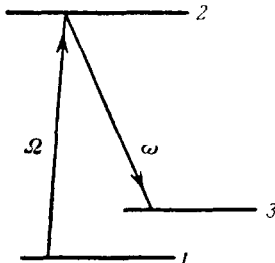


FIG. 3. Diagram of the transitions in Raman scattering.

the intermediate level (2) provides matrix elements $\mu_{1,2}$ and $\mu_{2,3}$ since $\mu_{1,3} = 0$. The polarization is given by the relation

$$\gamma = \sum_n \mu_{nk} Q_{kn} = \mu_{2,1} Q_{1,2} + \mu_{3,2} Q_{2,3} + \text{comp. conj.} \quad (31)$$

The equations of motion in the presence of the fields E_1 and E_2 are:

$$\left. \begin{aligned} \dot{Q}_{1,2} + \frac{Q_{1,2}}{T} - i\omega_{2,1} Q_{1,2} &= -\frac{i}{\hbar} \mu_{1,2} E (Q_{2,2} - Q_{1,1}) + \frac{i}{\hbar} \mu_{3,2} E Q_{1,3}, \\ \dot{Q}_{2,3} + \frac{Q_{2,3}}{T} - i\omega_{3,2} Q_{2,3} &= -\frac{i}{\hbar} \mu_{2,3} E (Q_{3,3} - Q_{2,2}) - \frac{i}{\hbar} \mu_{2,1} E Q_{1,3}, \\ \dot{Q}_{1,3} + \frac{Q_{1,3}}{T} - i\omega_{3,1} Q_{1,3} &= -\frac{i}{\hbar} \mu_{1,2} E Q_{2,3} + \frac{i}{\hbar} \mu_{2,3} E Q_{1,2}. \end{aligned} \right\} \quad (32)$$

Here

$$\omega_{i,j} = \frac{E_i - E_j}{\hbar}.$$

Thus for the energy level scheme of Fig. 3 the frequencies $\omega_{2,1}$ and $\omega_{3,1}$ are positive, and the frequency $\omega_{3,2}$ is negative. In these equations $\rho_{1,2}/T$ describes the decay of the matrix element connecting states 1 and 2, $(\rho_{2,2} - \rho_{1,1})$ is the population difference between the states 2 and 1, and the last term is the interaction between the states 1 and 3, etc. The electric field has the form

$$E = E_1 \cos(\omega t + \varphi_1) + E_2 \cos(\Omega t + \varphi_2). \quad (33)$$

If we neglect saturation, the solutions for $\rho_{1,2}$, $\rho_{2,3}$, and $\rho_{1,3}$ have the form

$$\left. \begin{aligned} Q_{1,2} &= \lambda_{1,2} e^{i\omega t} + \lambda_{1,2}^- e^{-i\omega t} + \Lambda_{1,3} e^{i\Omega t} + \Lambda_{1,2}^- e^{-i\Omega t}, \\ Q_{2,3} &= \lambda_{2,3} e^{i\omega t} + \lambda_{2,3}^- e^{-i\omega t} + \Lambda_{2,3} e^{i\Omega t} + \Lambda_{1,2}^- e^{-i\Omega t}, \\ Q_{1,3} &= D^+ e^{i(\Omega - \omega)t} + D^- e^{-i(\Omega - \omega)t}. \end{aligned} \right\} \quad (34)$$

The coefficients $\lambda_{1,2}^-$ and $\lambda_{2,3}^-$ are related to $\lambda_{1,2}$ and $\lambda_{2,3}$ by D^+ , since $\lambda_{1,2}$ and $\lambda_{2,3}$ are related to $\Lambda_{1,2}$ and $\Lambda_{2,3}$ via D^- . Furthermore putting $\Omega > \omega$ we find that the equation for $\rho_{1,3}$ has a resonance if $\Omega - \omega \approx \omega_{3,1}$, which causes the choice of the values ($\lambda_{1,2}^-$, $\lambda_{2,3}^-$, $\Lambda_{1,2}$ and $\Lambda_{2,3}$) to be much broader than the choice of the values ($\lambda_{1,2}$, $\lambda_{2,3}$, $\Lambda_{1,2}$, $\Lambda_{2,3}$). The complete expression for each choice are four inhomogeneous linear equations. These equations simplify if one assumes that $E_2 \gg E_1$. In this case we obtain the coefficients describing Raman scattering as follows:

$$\lambda_{1,2}^- = -i \left| \frac{\mu_{2,3} E_2}{2\hbar \Omega} \right|^2 \frac{\mu_{1,2}}{2\hbar} (Q_{2,2} - Q_{3,3}) \times T \frac{E_1}{-i[\omega_{3,1} - (\Omega - \omega)] + \frac{1}{T}}, \quad (35)$$

where it is assumed that $\Omega \gg \omega_{ij}$ and

$$\lambda_{2,3}^- = -i \left| \frac{\mu_{1,2} E_2}{2\hbar \Omega} \right|^2 \frac{\mu_{2,3}}{2\hbar} (Q_{1,1} - Q_{2,2}) \times T \frac{E_1}{-i[\omega_{3,1} - (\Omega - \omega)] + \frac{1}{T}}, \quad (36)$$

where it is assumed that Ω and ω are much larger than ω_{ij} .

The polarization is determined by the expression

$$\gamma = \mu_{2,1} \lambda_{1,2}^- + \mu_{3,2} \lambda_{2,3}^- + \text{comp. conj.} \quad (37)$$

If one uses the expressions for $\lambda_{1,2}^-$ and $\lambda_{2,3}^-$ in γ , the population of level 2 drops out. Thus γ is proportional to $(\rho_{1,1} - \rho_{3,3})$, which was to be expected from the previous discussion from the rate of photon emission.

The increase in power is given by

$$\Delta P = \frac{\omega}{2} \chi'' E_1^2 l, \quad (38)$$

where l is the sample length. From this, using the expression $\gamma = (\chi' + i\chi'')Ee^{i\omega t}$ we find

$$\chi'' = \left| \frac{\mu_{2,3} E_2}{2\hbar \Omega} \right|^2 \frac{|\mu_{1,2}|^2}{\hbar} T(\rho_{1,1} - \rho_{3,3}). \quad (39)$$

We note that for $\rho_{1,1} > \rho_{3,3}$, i.e., for positive temperatures, χ'' is positive and as a result E_1 is amplified.

The increase in the stimulated Raman scattering $\Delta P/P$ can be obtained by dividing the above expression for ΔP by $P = E_1^2 l$, which gives

$$G = \frac{\omega \chi''}{2}. \quad (40)$$

This expression may be given a more usual form. To do this we make the simplifying assumption that all atoms are in the state 1, i.e., $\rho_{3,3} = 0$. Further we assume that the quantity

$$A = \frac{\omega_{1,2}}{2} \frac{|\mu_{1,2}|^2 T \rho_{1,1}}{\hbar} \quad (41)$$

is the absorption coefficient for the applied field. This quantity may be measured directly. Thus

$$G = \frac{\omega}{\omega_{1,2}} \left| \frac{\mu_{2,3} E_2}{2\hbar \Omega} \right|^2 A. \quad (42)$$

In practice there may be several levels which play the role of intermediate states. The preceding discussion applies to the most important level, for which the absorption is greatest. In general it is necessary to sum over all intermediate states.

In a particular case, if the power is 1 MW or $E = 600$ cgs esu, and for an electric dipole moment of 1 Debye and for $\Omega = 10^{14}$ cps, the power gain has the form

$$G = \frac{\omega}{\omega_{1,2}} A \left| \frac{\mu E}{2\hbar \Omega} \right|^2 \approx \frac{\omega}{\omega_{1,2}} A \left| \frac{10^{-18} \cdot 600}{10^{-27} \cdot 6 \cdot 10^{14}} \right|^2 \approx \frac{\omega}{\omega_{1,2}} A \cdot 10^{-6}.$$

Thus in order to obtain a gain equal to unity it is necessary to have strong absorption at the frequency $\omega_{1,2}$.

For anti-Stokes lines the role of ω and Ω must be interchanged. At the same time we assume that initially there is a large field at frequency Ω . We then apply the second field at frequency ω_{AS} , where $\omega_{AS} > \Omega$ and $\omega_{AS} - \Omega \approx \omega_{3,1}$; then photons at the frequency ω_{AS} will be absorbed. Then as above we obtain

$$\gamma_{AS} = -i \left| \frac{\mu_{2,3} E_2}{2\hbar \Omega} \right|^2 \frac{|\mu_{1,2}|^2}{2\hbar} T E_{AS} (\rho_{1,1} - \rho_{3,3}). \quad (43)$$

Here E_{AS} is the amplitude of the field of the anti-

Stokes frequency. Thus this term in the Raman scattering always gives absorption if $\rho_{1,1} > \rho_{3,3}$.

However the same set of equations in the presence of fields at frequencies Ω and ω where $\Omega - \omega \approx \omega_{3,1}$ may cause the appearance of oscillating components γ at frequency $\Omega + \omega_{3,1}$. According to the above equation this effect may give rise to amplification of the anti-Stokes component in spite of absorption. This effect has the form of a resonant optical frequency shift.

We now write down the equations for the density matrix. With the simplifying assumptions that the temperature is low and that $\rho_{1,1} = 1$, $\rho_{2,2} = \rho_{3,3} = 0$, we obtain

$$\left. \begin{aligned} \dot{\rho}_{1,2} + \frac{\Omega_{2,1}}{T} - i\omega_{2,1}\rho_{1,2} &= \frac{i}{\hbar} \mu_{1,2} E Q_{1,1} + i\hbar \mu_{3,2} E Q_{1,3}, \\ \dot{\rho}_{2,3} + \frac{\Omega_{2,3}}{T} - i\omega_{3,2}\rho_{2,3} &= \frac{i}{\hbar} \mu_{3,2} E Q_{1,3}, \\ \dot{\rho}_{1,3} + \frac{\Omega_{1,3}}{T} - i\omega_{3,1}\rho_{1,3} &= -\frac{i}{\hbar} \mu_{1,2} E Q_{2,3} + \frac{i}{\hbar} \mu_{2,3} E Q_{1,2}. \end{aligned} \right\} (44)$$

Here

$$\begin{aligned} E &= E_1 \cos(\omega t + \varphi_1) + E_2 \cos(\Omega t + \varphi_2) \\ &= (E_1^+ e^{i\omega t} + E_1^- e^{-i\omega t}) + (E_2^+ e^{i\Omega t} + E_2^- e^{-i\Omega t}), \end{aligned} \quad (45)$$

where

$$E_1^\pm = \frac{1}{2} E_1 e^{\pm i\varphi_1}, \quad E_2^\pm = \frac{1}{2} E_2 e^{\pm i\varphi_2}.$$

Furthermore

$$\omega_{i,j} = \frac{E_i - E_j}{\hbar}.$$

We will assume that level 2 is far from the center of gravity of levels 1 and 3.

We note that the term $\lambda_{1,2}^- e^{-i\omega t}$ has a two-fold origin. One part of the coefficient $\lambda_{1,2}$ is discussed above and gives rise to the Raman scattering term. There is another part which arises from the usual resonance absorption in the wings due to the interaction of single quanta with levels 1 and 2. We write this term as $\Gamma_{1,2}^- e^{i\omega t}$. In this case the real part of $\Gamma_{1,2}^-$ is much larger than the imaginary part. This real part plays no role in the absorption of single quanta of frequency ω described here. Its value is

$$\Gamma_{1,2}^- = \frac{\mu_{1,2} \rho_{1,1} E_1^-}{\hbar (\omega + \omega_{2,1})}.$$

This expression may be obtained from the equation for $\dot{\rho}_{1,2}$ by neglecting the term proportional to $\rho_{1,3}$ and estimating the amplitude for the oscillating component $e^{-i\omega t}$. We note the simplifying assumption $\rho_{2,2} = \rho_{3,3} = 0$ gives $\Gamma_{2,3} = 0$, which is clear from the equation for $\dot{\rho}_{2,3}$. We note also that in the equation for $\dot{\rho}_{1,3}$ the quantity $\rho_{1,2}$ is related to E . This gives an oscillating term with frequency $\Omega - \omega$ in $\rho_{1,3}$. This term has a resonance for $\Omega - \omega \approx \omega_{3,1}$. Assume that such a resonance occurs. Then from $\dot{\rho}_{1,3}$ we obtain for the component of $\rho_{1,3}$ at frequency $\Omega - \omega \approx \omega_{3,1}$ the equation

$$Q_{1,3} = -\frac{i\mu_{1,2}\mu_{3,2}\rho_{1,1}\Gamma_{1,2}^-}{\hbar^2(\omega + \omega_{2,1})} E_2^+ E_1^- e^{i(\Omega - \omega)t}. \quad (46)$$

This component $\rho_{1,3}$ in equations for $\dot{\rho}_{1,2}$ and $\dot{\rho}_{2,3}$

gives rise to oscillating components of these two quantities at the frequency $2\Omega - \omega$, because of the connection between $\rho_{1,3}$ and E . As a result we have

$$Q_{1,2} = -\frac{i|\mu_{2,3}|^2\mu_{1,2}\Gamma}{\hbar^3(\omega+\omega_{2,1})(\Omega-\omega_{2,3})}E_2^+E_2^+E_2^-e^{i(2\Omega-\omega)t}, \quad (47)$$

$$Q_{2,3} = -\frac{i|\mu_{1,2}|^2\mu_{2,3}\Gamma}{\hbar^3(\omega+\omega_{2,1})(\Omega+\omega_{2,1})}E_2^+E_2^+E_2^-e^{i(2\Omega-\omega)t}, \quad (48)$$

$$\gamma = \mu_{2,1}Q_{1,2} + \mu_{3,2}Q_{2,3} + \text{comp. conj.};$$

γ is equal to the real part of the quantity

$$-i\frac{(\omega_{2,1}+\omega_{2,3})}{(\Omega+\omega_{2,1})(\Omega-\omega_{2,3})}\frac{2|\mu_{1,2}\mu_{2,3}|^2Q_{1,1}\Gamma}{\hbar^3(\omega+\omega_{2,1})}E_2^+E_2^+E_2^-e^{i(2\Omega-\omega)t}.$$

We note that if level 2 is located exactly halfway between levels 1 and 3, so that $\omega_{2,1} = -\omega_{2,3}$, the above expression becomes zero. However if level 2 is higher than level 3, $\omega_{2,1} \gg \omega_{3,1}$ and $\omega_{2,1}$ is comparable with Ω (for example Ω is of the order of $2\omega_{2,1}$), so that

$$\gamma = -\beta\frac{2i|\mu_{1,2}\mu_{2,3}|^2Q_{1,1}\Gamma}{\hbar^3\Omega^2}E_2^+E_2^+E_2^-e^{i(2\Omega-\omega)t}, \quad (49)$$

where under the above conditions β is of the order of unity.

This oscillating component can radiate at frequency $2\Omega - \omega$, equal to the frequency of the anti-Stokes line. For the anti-Stokes line generated by the field E_2 we have, as has already been shown above,

$$\gamma = -\beta\frac{2i|\mu_{1,2}\mu_{2,3}|^2Q_{1,1}\Gamma}{\hbar^3\Omega^2}E_2^2E_{as}e^{i(\Omega+\omega_{2,1})t}. \quad (50)$$

We note that if $E_2 \gg E_{as}$ then in the direction in which $2\varphi_2 - \varphi_1 = 0$ we obtain parametric amplification at the frequency $2\Omega - \omega = \Omega + \omega_{3,1}$ which is larger than the loss.

Similar effects may occur for higher order harmonics.

V. S. Mashkevich^[14] has given a theory of stimulated Raman scattering in the Stokes region based on kinetic equations. The author reaches the conclusion that in order to obtain sharp line oscillation in the "red" satellites it is desirable to use a cavity with maximum frequency dispersion. This allows one to pump over a frequency interval equal to the scattered line width.

C. Theoretical Calculation of Several Processes Involved in Stimulated Raman Scattering

Helwarth^[15,16] has made more detailed calculations allowing one to describe the time dependence of the growth of intensity of the stimulated Raman scattering and also the decrease in the width of the emitted Raman lines.

Helwarth treats the Raman active medium as being inside the cavity. The initial phase of the process of interest is characterized by the following conditions: a) there is a large number of photons n_α in each mode of the cavity close to the laser frequency ω_α ; b) in the laser medium the population inversion is reduced essentially to zero because of the formation of the giant

pulse and does not vary significantly during the Raman scattering; c) the Raman active medium is in thermodynamic equilibrium. Consequently the ruby does not take part in the succeeding stimulated Raman process; its absorption is included in the overall losses of the cavity. The optical modes of the cavity are described essentially by plane waves running in opposite directions with constant amplitude in a region of cross section a and amplitude zero outside this region. These modes propagate through the Raman active medium and cause the increase in the intensity of the frequency shifted radiation. Let g_β be the increase per centimeter of the radiation at frequency ω_β , with wave vector \mathbf{k}_β polarization \mathbf{e}_β . In what follows we will consider only the direction along the axis of the system.

If l is the length of the column of the scattering substance, (along the axis) and γ_β is the loss accompanying one pass of the beam through the resonator, then the condition for gain at frequency ω_β is

$$g_\beta l > \gamma_\beta. \quad (51)$$

Here the quantity τ/γ_β is the natural lifetime of modes close to the axis, and τ is the time for light to pass once through the cavity.

According to the theory of stimulated Raman scattering, the increase in the radiation intensity caused by plane waves of intensity I_α (photons/cm² sec) is

$$g_\beta = \sum_\alpha I_\alpha \sigma_{\alpha\beta} \lambda_\beta^4 \left[1 - \exp\left(-\frac{\hbar\Delta_{\alpha\beta}}{kT}\right) \right] c_\beta^{-1} [\text{cm}^{-1}]. \quad (52)$$

Here λ_β is the wavelength of the scattered light, C_β is the velocity of this wave in the medium, $\Delta_{\alpha\beta} = \omega_\alpha - \omega_\beta$, and $\sigma_{\alpha\beta}$ is the Raman scattering cross section per unit wavelength in the medium for a frequency change from ω_α to ω_β (calculated per steradian and per unit volume of the medium). For linearly polarized scattered light

$$\sigma_{\alpha\beta} = B \cos^2 \theta + C,$$

where θ is the angle between \mathbf{e}_α and \mathbf{e}_β ; B and C are quantities depending on ω_α and $\Delta_{\alpha\beta}$. Equation (52) is valid under the assumption of thermodynamic equilibrium, which holds in practice.

We now consider the way in which a photon makes the transition from the "incident" mode of the cavity α to the "scattered" mode β . The number of photons n_β in each scattered mode of the resonator must satisfy the condition

$$\frac{dn_\beta}{dt} = \frac{n_\beta}{\tau} (g_\beta l - \gamma_\beta). \quad (53)$$

This equation takes into account both the usual losses in the cavity and the stimulated Raman emission but it does not take account of the ordinary Raman scattering. The latter may be taken into account by replacing n_β by $n_\beta + 1$. This degree of precision is important only at the start ($t=0$), since at later instants of time $n_\beta \gg 1$. We can now construct the equations

for the time dependence of g_β . In doing this it is convenient to express g_β in terms of the number n_α of photons in each of the incident modes. If I'_α is the sum of the intensities of the waves propagating to the left and to the right, then $n_\alpha = I'_\alpha a$. We then obtain from (52)

$$g_\beta = \sum_\alpha \sigma_{\alpha\beta} n_\alpha \lambda_\beta^4 \left[1 - \exp\left(-\frac{h\Delta_{\alpha\beta}}{kT}\right) \right] / c_\beta \tau a, \quad (54)$$

$$\frac{dn_\beta}{dt} = n_\beta \left(\sum_\alpha n_\alpha G_{\alpha\beta} - \omega_\beta \right), \quad (55)$$

Here

$$G_{\alpha\beta} = \sigma_{\alpha\beta} \lambda_\beta^4 \left[1 - \exp\left(-\frac{h\Delta_{\alpha\beta}}{kT}\right) \right] l / c_\beta \tau^2 a. \quad (56)$$

Here $w_\beta (\equiv \gamma_\beta / \tau)$ is the natural decay rate of the cavity modes β . The sum over the incident modes α in (55) means that photons from the modes α of the cavity scatter into the modes β ; it follows from this that

$$\frac{dn_\alpha}{dt} = -n_\alpha \left(\sum_\beta n_\beta G_{\alpha\beta} + \omega_\alpha \right). \quad (57)$$

Equations (55)–(57) describe stimulated Raman scattering. Because of the great difficulty in solving this system of equations we will consider two limiting cases.

The case of scattering of a small fraction of the incident photons. In the majority of experiments in which stimulated Raman scattering is observed, only a small fraction (10^{-3} – 10^{-1}) of the incident photons are actually scattered. Because of this the number of incident photons $X(t) = \sum_\alpha n_\alpha$ decreases only because of the normal damping $X_0 \exp(-wt)$. In this case integration of the system (55) gives

$$n_\beta = \eta \exp \left[\frac{G_\beta X_0 (1 - e^{-wt})}{w} - \omega_\beta t \right]. \quad (58)$$

Here X_0 is the total number of photons initially present in the giant pulse, and

$$\eta = \left\{ 1 - \exp\left(-\frac{h\omega_\beta}{kT}\right) \right\}^{-1}$$

is the number of photons originally present in each mode β . For vibrational transitions in molecules $\eta \approx 1$. Since each mode α has the same effect we have $G_{\alpha\beta} = G_\beta$. It is clear from (58) that the ratio r_β of the initial growth in the modes β to the losses in the modes α should satisfy the condition

$$r_\beta = \frac{G_\beta X_0}{w} \gg \frac{\omega_\beta}{w}, \quad (59)$$

which permits a very large increase before the number of incident photons dies out.

We now calculate the total instantaneous scattered power

$$\Phi(t) \equiv \sum_\beta \omega_\beta (n_\beta - \eta)$$

(photons/sec) in the mode β . Until the instant at which

Φ has grown sufficiently to give an appreciable signal, $r_\beta (1 - e^{-wt})$ is so large that the limiting approximation in the sum over β is very accurate. In this connection we take $r_\beta \approx r(1 - \delta^2)$, where for a dispersion line δ is the displacement of the frequency of the mode β from the center of the line in units of the half-width of the line. The modes may be considered to be distributed uniformly with a density ρ . It follows from (58) (assuming $w_\beta = W = \text{const}$) that

$$\Phi(t) \rightarrow W \rho \eta \pi^{1/2} [r(1 - e^{-wt})]^{-1/2} \exp[r(1 - e^{-wt}) - Wt]. \quad (60)$$

This expression applies to times immediately after the beginning of the scattering (i.e., for $wt > r^{-1}$). The output power has a spike at time t_m , which may be calculated approximately from the condition

$$\omega t_m = \ln \left(\frac{rw}{W} \right) \quad (61)$$

and may be as long as several time constants w^{-1} , since for appreciable laser action $r \gg W/w$. This means that the value of the output power in the spike is approximately

$$\Phi_m \approx W \rho \eta \left(\frac{W}{wr} \right)^{W/w} e^{r - W/w} \left(\frac{\pi}{r} \right)^{1/2}. \quad (62)$$

[In (60) we have made the approximation of replacing the factor $[1 - \exp(-wt)]^{-1/2}$ by unity.] Curves of the dependence of Φ on $(wr - \ln r)$ (for several values of the parameter W/w) are given in Fig. 4. Experimentally one is interested in the quantity ξ_β , the fraction of the initial photons X_0 which are scattered into the modes β at various deviations from the center of the line, and one is also interested in $\sum_\beta \xi_\beta$, which is proportional to the integrated line intensity at ω_β . Ac-

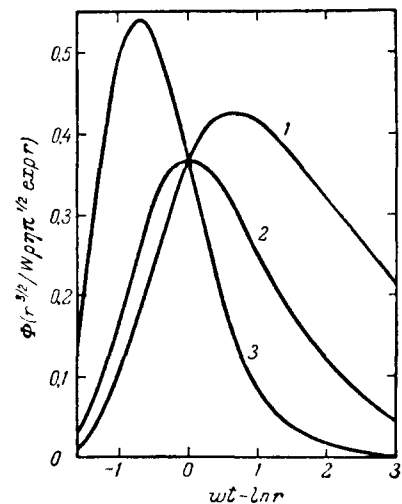


FIG. 4. Plot of Eq. (60) for the scattered power Φ as a function of $wt - \ln r$. w is the natural decay rate of the mode of the incident light, r is the ratio of the peak of the initial increase in Raman scattering $X_0 G$ to the losses w of the incident mode. Curves 1, 2, and 3 correspond to $W/w = 1/2, 1, 2$, where W is the natural damping rate of the scattered modes.

ording to (55) we have

$$\xi_{\beta} = G_{\beta} \int_0^{\infty} n_{\beta}(s) \frac{X(s)}{X_0} ds. \quad (63)$$

Keeping (58) in mind and making the change of variable $v = re^{-wt}$, we have

$$\xi_{\beta} = \eta r_{\beta}^{-W/w} e^{r_{\beta}} \int_0^r e^{-v} \frac{v^{W/w}}{X_0} dv. \quad (64)$$

For appreciable scattering we have $W/w \ll r$. It follows that for the most important modes, close to the center of the line, the integrand in (64) for $v = r$ is so small that the upper limit may be replaced by ∞ . Consequently

$$\xi_{\beta} = r_{\beta}^{-W/w} X_0^{-1} \Gamma\left(1 + \frac{W}{w}\right) \exp(-r_{\beta}), \quad (65)$$

where $\Gamma(x)$ is the gamma function. It is clear from this that the half-width of the scattered line is narrowed in comparison to the ordinary Raman scattered line by a factor $\delta_{1/2}$, where

$$\delta_{1/2} = \left(\frac{\ln 2}{r}\right)^{1/2} \quad (66)$$

(each mode, of course, emits an extremely narrow line).

We now consider the case in which a significantly large fraction of the incident photons is scattered (up to 30% in experiments with nitrobenzene). In this case the previous treatment will not be suitable because of the great sensitivity of the solutions of (55) and (57) to small changes in either w_{β} or G_{β} . Moreover the whole idea of separate modes loses its meaning since there is significant growth of the power in the mode during the very short duration of the light pulse in the resonator and the modes overlap.

We transform Eqs. (55)–(57), assuming that the losses are the same for all photons ($w_{\beta} = W$) and that the gains are the same ($G_{\beta} = G$). Designating the total number of scattered photons by $Y(t)$, we write

$$\frac{dY}{dt} = Y(XG - W), \quad (67)$$

$$\frac{dX}{dt} = -X(YG + w), \quad (68)$$

where G is the peak value obtained from (56). The initial value is presumably the number of thermal photons present in the modes.

Dividing (67) by (68) and integrating the result we find

$$(X - X_0 + Y - Y_0) G \frac{w}{W} = \ln \left(\frac{XY_0}{YX_0} \right). \quad (69)$$

From this result one may in principle obtain $X(Y)$ and, putting this in (68), one may find $X(t)$. In view of the mathematical difficulties, however, we limit ourselves to the optimal and most interesting case, in which $w = W$. In this case we have from (67) and (68)

$$X + Y = (X_0 + Y_0) e^{-wt}, \quad (70)$$

which with (69) gives

$$Y = be^{-wt} \left\{ 1 + d \exp \left[\frac{Gb(e^{-wt}-1)}{w} \right] \right\}^{-1}, \quad (71)$$

where $b = X_0 + Y_0$ and $d = X_0/Y_0$. This solution, for $X_0G/w = 40$, $d = 10^{15}$ is shown in Fig. 5. The graph of $X(t)$ is shown in the same figure. As may be seen $X(t)$ falls off exponentially as $X_0 \exp(-wt)$, while $Y(t)$ goes from comparatively small values to a maximum. Then $X(t)$ abruptly falls approximately to zero, since all of the photons which were originally in the exciter light have been transferred to the scattered light. The scattered light then falls off exponentially. It follows from (71) that the time t_n for obtaining the maximum scattering obeys the same condition (61) as in the case of weak scattering. An estimate of the spectral width of the output line gives the same result as in the case of weak scattering [cf. (66)]. In this respect the two limiting cases give similar results. Numerical estimates made on the basis of the above theory give results in good agreement with the experimental data for nitrobenzene.

4. OPTICAL MASERS UTILIZING STIMULATED RAMAN SCATTERING OF LIGHT

The experimental and theoretical papers discussed above showed that stimulated Raman scattering can be expected to be widely useful in transforming laser radiation from one spectral region to another. Moreover a variety of optical masers may be constructed using stimulated Raman scattering.

As mentioned above, the experimental investigations of stimulated Raman scattering used a ruby laser as the source of stimulating radiation. This was necessary because the threshold for stimulated Raman scat-

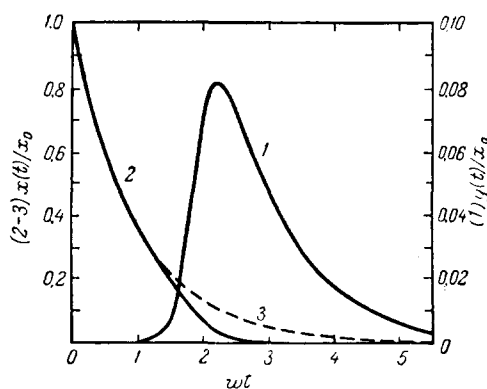


FIG. 5. Curve 1 (right-hand ordinate) is a graph of Eq. (71) for the ratio of the number of scattered photons to the initial number of photons in the exciting pulse Y/X_0 as a function of wt for a value of the parameter $d = X_0/Y_0 = 10^{15}$. Curve 2 (left-hand ordinate) gives the ratio of the number of exciting photons to the initial number of photons X/X_0 as a function of wt . Curve 3 shows the behavior of X/X_0 as a function of wt in the absence of stimulated Raman scattering.

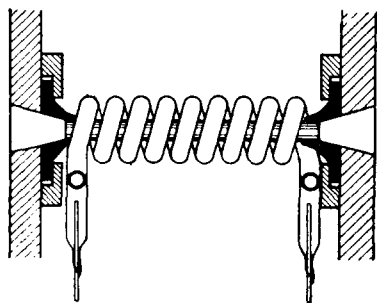


FIG. 6. Experimental set-up for observing inverted Raman spectra.

tering is quite high, i.e., energy densities of the order of $1,000 \text{ (watts/cm}^2\text{)/cm}^{-1}$ are necessary and may be obtained from other radiation sources only with great difficulty. However it is of course true that it is in principle completely possible to obtain stimulated Raman scattering using "ordinary" excitation sources.

A paper by Becker^[18] has appeared quite recently in which an experiment was undertaken to obtain optical maser action using the principle of Raman scattering. The experimental arrangement used in this experiment is shown schematically in Fig. 6. The material investigated was α -quartz. The sample of α -quartz was prepared in the form of a cylinder with polished ends. The ends were polished to the surface-parallelism and flatness specifications customary for optical masers. The cylinder was cut so that its axis coincided with the symmetry axis of the crystal. The source of exciter radiation was a specially prepared high powered spiral quartz lamp with electrodes of liquid mercury. The lamp was pumped out in a high vacuum. The lamp was pulsed to obtain the maximum light output power. The electrical energy for the lamp was stored in high-voltage capacitors. The apparatus provided electrical discharges with energies from 0.25–250 joules. Under these conditions the maximum electrical power in the discharge was 20 megawatts. The emission was recorded on a spectrograph especially prepared for this purpose which included a quartz spectrograph and a rotating table. The rotating table permitted one to vary the position of the symmetry axis of the sample with respect to the axis of the spectrograph, which made it possible to decrease substantially the fraction of parasitic ultraviolet radiation falling on the spectrograph. Under these conditions the author succeeded in studying the lines of α -quartz in the range from 93 to 1500 cm^{-1} . The maximum efficiency of the apparatus was obtained using photoelectric recording. In this case the entrance slit of the photomultiplier coincided with the focal plane of the camera.

An investigation was made of the dependence of the ratio of the intensities of the Stokes and anti-Stokes Raman lines on pump energy. The Raman scattering was excited by the ultraviolet lines of mercury at 2537 and 3650 Å. The author was able to vary the pump en-

ergy within wide limits. In exciting the Raman spectra with the 2537 Å line the pump energy varied from 6 to 100 joules; when the 3650 Å line was used the energy varied from 0.25 to 15 joules.

It is known from theory (cf. for example^[12]) that under normal conditions the ratio of the intensities of the anti-Stokes lines I_{as} to the Stokes lines I_s is always less than unity. The author observed an anomalous effect, i.e., $I_{as}/I_s > 1$. This inversion effect was observed not only in the lines at the fundamental frequencies but also in the overtones and combination frequencies. Inversion was observed in more than 70 lines in all. In Fig. 7a we show schematically the ordinary (i.e., for small flash-lamp energies) spectrum of the Raman scattering from α -quartz. Even under these conditions one finds several lines for which I_{as}/I_s is larger than unity. The author explains this by the fact that the duration of the flash is small and the molecules cannot follow the pumping intensity because of anharmonicity. In Fig. 7b we show the form of the spectrum for large pumping energies. It is clear from the figure that all of the anti-Stokes lines have larger intensities than the Stokes lines. It was found during the experiment that the 3650 Å line was more effective. For example, for a pumping energy of 6 joules the Raman spectrum excited by the 3650 Å line

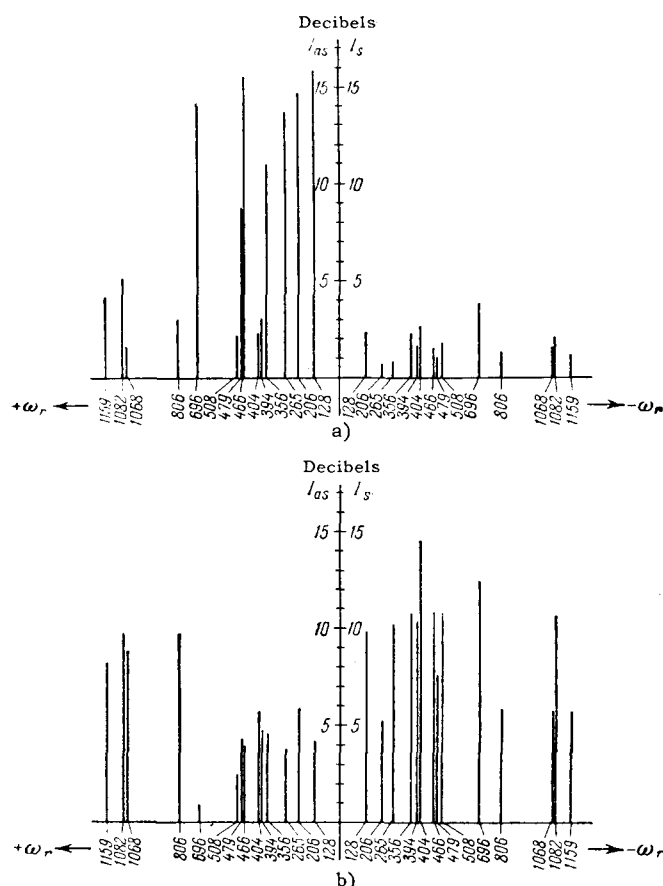


FIG. 7. The Raman spectra of α -quartz (fundamental vibrations) obtained under pulsed excitation: a) inverted, b) ordinary spectrum.

is completely inverted, whereas the spectrum obtained from the 2537 Å line has the normal appearance. The author observed that the inversion effect appeared when a definite threshold was obtained and moreover that this threshold was very sharp (changing the voltage on the condenser bank by 10% led to complete inversion of the spectrum). It should be pointed out that this experiment was carried out without the use of resonator.

In order to explain these results the author investigated theoretically the possibility of causing optical maser action using Raman scattering. Starting from the theory of Plachek^[12] and using his methods, Becker obtained^[18] expressions for the transition probabilities per unit time at the characteristic vibrational frequencies of the molecules and at the anti-Stokes frequencies. From an analysis of these expressions the author reached the conclusion that it is in principle possible to make an optical maser using the Raman effect. The physical picture of this phenomenon is essentially the same as that given by Townes et al. (cf. Sec. 3).

Considering the well known expression for the ratio of the intensities of anti-Stokes to Stokes lines in Raman scattering

$$\frac{I_{as}}{I_s} = \frac{N_+}{N_0} \left(\frac{\omega_0 + \omega_r}{\omega_0 - \omega_r} \right)^4,$$

(where ω_0 and ω_r are the frequencies of the exciting radiation and the molecular vibration respectively, and N_+/N_0 is the ratio of the populations in the excited and unexcited states) the author concluded that inversion could be obtained only when the temperature of the system was negative. Under ordinary conditions the ratio N_+/N_0 obeys the Boltzmann distribution, i.e.,

$$\frac{N_+}{N_0} = e^{-\frac{h\nu_r}{kT}}.$$

Thus under ordinary conditions I_{as}/I_s is always less than unity. Hence $I_{as}/I_s > 1$ may be obtained only if the system exhibits population inversion, i.e., if $T < 0$. The author^[18] considers his experiment to prove the presence of population inversion and thus to open up the possibility of laser action at frequency ω_r .

The results of this paper are very interesting but should, we think, be approached with caution. For example, the author maintains that he observed a quantum mechanical amplification of the order of 25 dB for the anti-Stokes lines of 1230 and 1398 cm^{-1} (third harmonic of the frequency 466 cm^{-1}). However in order to observe gain at any frequency it is necessary that radiation be present at this frequency. The author explains that the Stokes line with frequency 1230 cm^{-1} overlaps the mercury line at 28622 cm^{-1} , i.e., the condition is fulfilled for this line. However the anti-Stokes line with frequency 1398 cm^{-1} does not correspond with any observed ultraviolet radiation and hence gain at this frequency is unexplained.

The feasibility of optical masers (including lasers in the infrared) operating on the basis of stimulated

Raman emission has been discussed elsewhere by other authors, for example by Townes^[10], and Javan^[13]. Moreover Loudon^[19] investigated theoretically the possibility of making optical masers operating on the vibrations of the crystal lattice. He obtained a theoretical expression for the laser threshold. Numerical calculations from this formula give $n_0 > (1 - R) \times 2 \times 10^{26}$ photons per cm^3 , where n_0 is the number of exciting photons, R is the reflectivity of the mirrors, taking all losses in the cavity into account. Similar calculations were made by Zeiger^[17]. The magnitude of the threshold determined by Zeiger was somewhat greater than found by Loudon.

In conclusion we note that the study of stimulated Raman scattering is developing extremely rapidly. Doubtless further work will afford a more thorough understanding of the phenomenon and will elucidate the possibilities for its practical application.

Note added in proof. Since this review went to press a number of new papers on stimulated Raman emission have appeared. References^[20, 21] treat a series of questions on the theory of two-photon processes, including in particular processes occurring in lasers operating via stimulated Raman scattering. Both papers derive expressions for the threshold for Raman laser action. Reference^[22] deals with the experimental testing of several contradictory ideas in the papers of Terhune^[7] and Zeiger and Tannenwald^[17], involving the angular distribution of the radiation from a Raman laser. Two papers^[23, 24] report Raman laser action in new materials. Eckhart et al.^[23] obtained laser action in the Raman lines of diamond, calcite and α -sulfur. Mink and co-workers investigated laser action in hydrogen, deuterium and methane. Laser action was obtained in the spectral region from 6000 to 30,950 cm^{-1} . Also, we have recently succeeded in observing stimulated Raman scattering in several organic liquids.

¹ L. I. Mandel'shtam, Coll. Works, vol. 1, p. 293, AN SSSR (1948); G. S. Landsberg, Selected Works, p. 355, AN SSSR (1958).

² E. J. Woodbury and W. K. Ng, Proc. IRE 50, 2367 (1962).

³ A. Javan, Bull. Amer. Phys. Soc. 3, 213 (1958); J. phys. radium 19, 806 (1958).

⁴ Eckhart, Hellwarth, McClung, Schwarz, Weiner, and Woodbury, Phys. Rev. Letts. 9, 455 (1962); Electronic Design 11, 28 (1963).

⁵ Geller, Bortfeld, and Sooy, Appl. Phys. Letts 3, 36 (1963).

⁶ Geller, Bortfeld, Sooy, and Woodbury, Proc. JEEE 51, 1236 (1963).

⁷ R. W. Terhune, Bull. Amer. Phys. Soc. 8, 359 (1963); A. Shawlow, Scientific American 209(1), 34 (1963).

⁸ B. P. Stoicheff, International School of Physics "Enrico Fermi," XXXI Course, August 19-31, 1963.

⁹ Garmire, Pandarese, and Townes, Phys. Rev. Letts. 11, 160 (1963).

¹⁰ C. H. Townes, International School of Physics "Enrico Fermi," XXXI Course, August 19-31, 1963.

- ¹¹G. Rivoire and R. Dupeyrat, *Comp. rend.* **256**, 1947 (1963).
- ¹²G. Plachek, *Rayleigh Scattering and the Raman Effect* (Russ. Transl.) Khar'khov (1935).
- ¹³A. Javan, International School of Physics "Enrico Fermi," XXXI Course, August 19-31, 1963.
- ¹⁴V. S. Mashkevich, *Ukr. Fiz. Zh. (Ukrainian Journ. Phys.)* **8**, 1035 (1963).
- ¹⁵R. W. Hellwarth, *Phys. Rev.* **130**, 1850 (1963).
- ¹⁶R. W. Hellwarth, *Appl. Optics* **2**, 847 (1963).
- ¹⁷H. J. Zieger and P. E. Tannenwald, *Proc. Third Quantum Electronic Conference, Paris, 1963*, p. 209.
- ¹⁸C. H. Bekker, *Z. Physik* **172**, 125 (1963).
- ¹⁹R. Loudon, *Proc. Phys. Soc.* **82**, 393 (1963).
- ²⁰V. T. Platonenko and R. V. Khokhlov, *JETP* **46**, 555 (1964), *Soviet Phys. JETP* **19**, 378 (1964).
- ²¹V. M. Faïn and E. G. Yashchin, *JETP* **46**, 695 (1964), *Soviet Phys. JETP* **19**, 474 (1964).
- ²²Zeiger, Tannenwald, Kern, and Herendeen, *Phys. Rev. Letts.* **7**, 419 (1963).
- ²³Eckhart, Bortfeld, and Geller, *Appl. Phys. Letts.* **3**, 137 (1963).
- ²⁴Mink, Terhune, and Rado, *Appl. Phys. Letts.* **3**, 181 (1963).

Translated by J. A. Armstrong

25